Extreme stiffness systems due to negative stiffness elements

Y. C. Wang
Department of Engineering Physics and Engineering Mechanics Program, University of Wisconsin–Madison, 147 Engineering Research Building, 1500 Engineering Drive, Madison, Wisconsin 53706-1687

R. S. Lakes[a)]
Department of Engineering Physics, Engineering Mechanics Program, Biomedical Engineering Department, Materials Science Program, and Rheology Research Center, University of Wisconsin–Madison, 147 Engineering Research Building, 1500 Engineering Drive, Madison, Wisconsin 53706-1687

(Received 15 October 2002; accepted 22 August 2003)

When an elastic object is pressed, we expect it to resist by exerting a restoring force. A reversal of this force corresponds to negative stiffness. If we combine elements with positive and negative stiffness in a composite, it is possible to achieve stiffness greater than (or less than) that of any of the constituents. This behavior violates established bounds that tacitly assume that each phase has positive stiffness. Extreme composite behavior has been experimentally demonstrated in a lumped system using a buckled tube to achieve negative stiffness and in a composite material in the vicinity of a phase transformation of one of the constituents. In the context of a composite system, extreme refers to a physical property greater than either constituent. We consider a simple spring model with pre-load to achieve negative stiffness. When suitably tuned to balance positive and negative stiffness, the system shows a critical equilibrium point giving rise to extreme overall stiffness. A stability analysis of a viscous damped system containing negative stiffness springs reveals that the system is stable when tuned for high compliance, but metastable when tuned for high stiffness. The metastability of the extreme system is analogous to that of diamond. The frequency response of the viscous damped system shows that the overall stiffness increases with frequency and goes to infinity when one constituent has a suitable negative stiffness.
[DOI: 10.1119/1.1619140]

I. INTRODUCTION

Press on a spring or a seat cushion. Observe the force required to achieve a given deformation. Stiffness refers to the ratio of the generalized force to the generalized displacement. For a spring the stiffness is the ratio of the force to the displacement: the usual spring constant k. For a three-dimensional solid viewed as a continuum in the context of elasticity theory,[1] the measure of stiffness is the ratio of the stress (force per area) to the strain (displacement per length), referred to as a modulus. For example, Young's modulus and the shear modulus are used for axial and torsional properties, respectively. Modulus is a continuum property independent of the geometry and size of the material.

Objects usually resist deformation by a restoring force. Positive stiffness occurs when the deformation is in the same direction as the applied force, corresponding to a restoring force that returns the deformable body to its neutral position. A negative stiffness object assists the imposed deformation. Negative stiffness involves a reversal of the usual directional relationship between force and displacement in deformed objects.

Negative stiffness is possible in systems with a pre-load. To demonstrate negative stiffness, compress a plastic ruler so that it forms a buckled S shape. Because a third force will presently be needed, the ruler's ends can be held in place by two books. This buckled shape is unstable, so hold it in place at the center inflection point. Then release the constraint, and observe the ruler suddenly snap to a new shape. This snap-through instability is indicative of negative stiffness.[2] One can also provide two constraints (such as two fingers) spaced by a small distance as shown in Fig. 1(a) and observe the ruler snap from one to the other geometrical configuration upon movement of the contact point. To demonstrate the negative stiffness of the S-shape ruler, constrain the center inflection point by pressing it with a spring or a deformable ring. As you move the free end of the spring, observe how the contact point moves. The direction of deformation of the spring or ring reveals whether the buckled ruler resists the imposed deformation or assists it. This demonstration reveals the existence of negative stiffness, its instability, and the possibility of stabilizing it by a constraint.

Buckled tubes also exhibit negative incremental stiffness, that is, the stiffness of a material to perturbations about a deformed configuration. Snap through[3] also occurs on the atomic scale in materials such as ferroelastic solids which exhibit a solid to solid phase transformation.

Negative stiffness is to be distinguished from a negative Poisson ratio. Poisson's ratio, denoted as ν, is defined as the negative lateral strain of a stressed body divided by its longitudinal strain. Based on the assumption of positive definiteness of the strain energy for isotropic and homogeneous solids, ν ranges from -1 to 0.5, which implies stability. Positive definiteness does not specify the particular value of Poisson's ratio within that range. The value of ν for most solid materials is between 0.25 and 0.33. Recently, foams with ν as small as -0.8 have been made and analyzed.[4,5] When ν is negative, materials become fatter in cross section when they are stretched. The stiffness of these foams is nevertheless positive.

Composite materials with negative stiffness constituents and exhibiting extreme mechanical properties have been reported in several theoretical and experimental studies.[6–9] The rationale for expecting extreme behavior in systems with one negative stiffness phase can be understood by considering the following thought experiments based on simple mechani-

cal spring models. For a parallel elastic system, $E_c = E_1 V_1 + E_2 V_2$, where E_c, E_1, and E_2 refer to the Young's modulus of the composite, phase 1, and phase 2, respectively. V_1 and V_2 refer to the volume fraction of phase 1 and phase 2 with $V_1 + V_2 = 1$. The parallel elastic system has bonded phases which undergo the same strain and is known as the Voigt model.[10] If we have parallel springs of spring constant k, then $k_c = k_1 + k_2$. Similarly, for a series system of springs, $k_c = 1/(k_1^{-1} + k_2^{-1})$. The system of springs in series is analogous to the Reuss model in composites.[10] In the series system, we can express the compliance $j = 1/k$ as $j_c = j_1 + j_2$. If one stiffness is negative, the corresponding compliance is negative. We can sum a positive and negative compliance to obtain a zero compliance and hence an infinite stiffness. Therefore, extreme, and even singular stiffness is possible in heterogeneous systems with a negative stiffness constituent. However, a negative stiffness element by itself is unstable, and the series model also is unstable. If systems containing negative stiffness can be made stable, they can be useful as a result of the unexpected large values of their physical properties.

A material with negative stiffness is in unstable equilibrium, because the material has a higher positive stored energy at equilibrium, compared to neighboring possible equilibrium configurations. A material with negative stiffness can be stable if it is constrained. For example, the buckled ruler is an example of such a stabilizing constraint. Also, a buckled rubber tube has a negative stiffness component,[6] and experimentally reveals a large peak in the mechanical damping, consistent with the prediction of the Reuss model with one phase having negative stiffness. Mechanical damping is the dominating mechanism in energy dissipation of a vibrating object. The idea that negative stiffness may occur has motivated a series of explorations of extreme phenomena in composite materials. An analytical model of a distributed composite shows[7] that isotropic composites can possess extreme stiffness and damping. Furthermore, the contribution of negative stiffness to physical properties of materials gives extremely large coupling effects, such as piezoelectric, pyroelectric, and thermal expansion coefficients.[11] In this article, we analyze the stability of several spring systems with a negative stiffness element.

II. STABILITY ANALYSIS WITH THE DEMONSTRATION OF A NEGATIVE STIFFNESS ELEMENT

A stability analysis can be done using two different approaches. One approach is to investigate the energy landscape of the system. This approach is only suitable for systems without energy dissipation. A region with a concave up energy profile, that is, the second derivative of the energy function is greater than zero, indicates that the system is locally stable around the equilibrium position.[12] An alternative method is to examine the eigenvalues of the perturbed dynamical system in the context of Lyapunov's stability theorem.[12,13] This approach allows the effects of dissipation, stored energy, and input power to be accommodated. Lyapunov's indirect method will be adopted here for a system with nonconservative components.

Lyapunov's indirect method often is called the Routh–Hurwitz criterion in electrical engineering.[13,14] This type of stability analysis is used to analyze electronic circuits that contain elements such as capacitors which store energy, and amplifiers. The method predicts the stability of a dynamic system, governed by

$$\dot{\mathbf{x}} = \mathbf{X}(\mathbf{x}), \tag{1}$$

where $\mathbf{X}$ is a column-vector function of $\mathbf{x}$, $\mathbf{x} = \mathbf{x}(t)$ is a column-vector function of time, and the dot denotes differentiation with respect to time. Using the calculus of variations the perturbation of the dynamical system can be written to first order as

$$\frac{d}{dt}(\delta \mathbf{x}) = \mathbf{J}|_{\mathbf{x}_e} \cdot \delta \mathbf{x}, \tag{2}$$

where the Jacobian matrix $\mathbf{J} = \partial \mathbf{X}/\partial \mathbf{x}$, or $J_{ij} = \partial X_i / \partial x_j$. The subscript $\mathbf{x}_e$ indicates that the matrix, $\mathbf{J}$, is evaluated at the equilibrium point $(d\mathbf{x}/dt = 0)$, $\mathbf{x} = \mathbf{x}_e$, where $\mathbf{X}(\mathbf{x}_e) = 0$.

Lyapunov's indirect method states that if all the roots of the characteristic equation of the matrix $\mathbf{J}$ of the perturbed system in Eq. (2) have negative real parts, then the unperturbed system, Eq. (1), is asymptotically stable.[14] However, when the real parts of the eigenvalues are zero, we need to investigate the imaginary part of the eigenvalues or the reduction in the eigenspace of the system. In this case the system will be stable when the imaginary part is nonzero.[15]

To demonstrate the relation between Lyapunov's indirect method and known cases of stability and instability, we first analyze a spring system with a negative stiffness element [see Fig. 1(b)]. The negative stiffness arises from a compressive pre-load in the springs. The equation of motion for the system is

$$m\ddot{x} + 2\left[kh\left(\frac{1}{\cos\alpha} - 1\right) + f^0\right]\sin\alpha = F, \tag{3}$$

where $x = x(t)$, and $\alpha = \alpha(t)$ [see Fig. 1(b)]. The symbol f^0 represents the pre-load inside both the *ac* and *bc* springs and should be distinguished from the applied force, F. If we replace the displacement x by the generalized coordinate α, we can express the equation of motion as

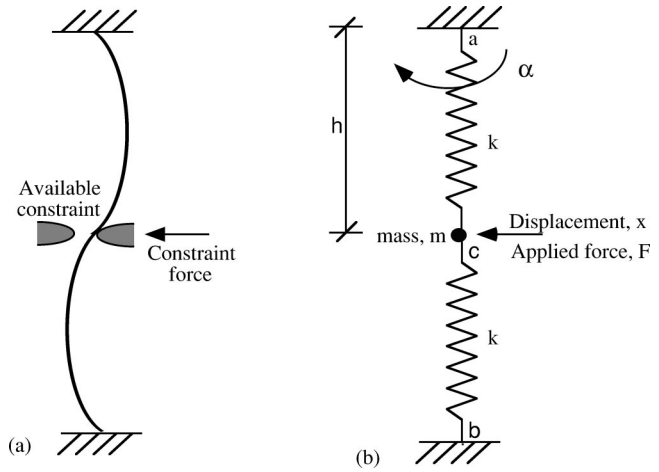

Fig. 1. (a) Buckled plastic ruler to demonstrate negative stiffness. (b). A spring system that can exhibit positive or negative stiffness depending on the pre-load. The symbol k represents the spring constant, the angle α the generalized coordinate describing the motion of the springs, and f^0 (not shown) the initial force in each spring.

$$(mh\sec^2\alpha)\ddot{\alpha}+(2mh\sec^2\alpha\tan\alpha)\dot{\alpha}^2+2kh\tan\alpha$$
$$-2kh\sin\alpha+2f^0\sin\alpha=F. \tag{4}$$

To investigate the stability around $\alpha\ll 1$ (corresponding to a vertical position of the springs) and $d\alpha/dt\ll 1$ with $F=0$, Eq. (4) can be further simplified:

$$\ddot{\alpha}+\frac{2f^0}{mh}\alpha=0. \tag{5}$$

To obtain the general form of the equation of motion for a dynamical system, as in Eq. (1), the standard method, which is called the state-space technique for reducing higher order ordinary differential equations to lower order ones, is used so that Eq. (5) can be rewritten as follows.[15] The first step in using Lyapunov's indirect method to investigate the stability is to change a higher order differential equation to a system of first-order differential equations:

$$\begin{pmatrix}\dot{\alpha}\\ \dot{q}\end{pmatrix}=\begin{bmatrix}0 & 1\\ -\frac{2f^0}{mh} & 0\end{bmatrix}\begin{pmatrix}\alpha\\ q\end{pmatrix}, \tag{6}$$

where $q=d\alpha/dt$. Near the equilibrium point, $\alpha=0$ and $q=0$, and $\mathbf{J}$ is

$$\mathbf{J}|_{\mathbf{x}_e}=\begin{bmatrix}0 & 1\\ -\frac{2f^0}{mh} & 0\end{bmatrix}. \tag{7}$$

The characteristic equation of $\mathbf{J}$ is

$$\lambda^2+\frac{2f^0}{mh}=0, \tag{8}$$

and hence,

$$\lambda_1=\sqrt{\frac{2|f^0|}{mh}}+i0, \tag{9a}$$

$$\lambda_2=-\sqrt{\frac{2|f^0|}{mh}}+i0, \tag{9b}$$

for $f^0<0$ (pre-compressed), and

$$\lambda_1=0+i\sqrt{\frac{2f^0}{mh}}, \tag{10a}$$

$$\lambda_2=0-i\sqrt{\frac{2f^0}{mh}}, \tag{10b}$$

for $f^0>0$ (pre-stretched), where λ represents the eigenvalues of $\mathbf{J}$. We conclude that the system is unstable when $f^0<0$, because $\mathrm{Re}(\lambda_1)>0$ in Eq. (9a), and is stable when $f^0>0$, because $\mathrm{Re}(\lambda_1)=\mathrm{Re}(\lambda_2)=0$ in Eq. (10) with nonzero imaginary parts. Note that the magnitude of the eigenvalues will be extremely large when the mass m approaches zero. The eigenvalues with large positive real parts cause the system to diverge rapidly from unstable equilibrium when the mass is small. Physically, it is understood that the system is locally stable in a pre-stretched state (that is, tensile pre-load) like a guitar string, but cannot be locally stable in a pre-compressed state (that is, a compressional pre-load).

If we perform the stability analysis by the energy method,[16] the total energy and its second derivative can be expressed as

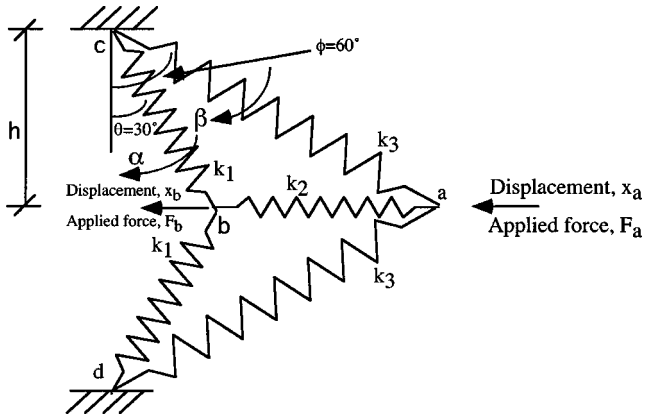

Fig. 2. Two-dimensional spring system, undeformed configuration. The angles α and β are generalized coordinates. The spring elements k_1, k_2, and k_3, may have initial forces, denoted as f_1^0, f_2^0, and f_3^0 (not shown), and changes of length, Δ_1, Δ_2, and Δ_3 (not shown). The structure is symmetric in loading conditions, geometry, and material properties. We may apply a force F_a, but $F_b=0$ throughout.

$$U=kh^2(\sec\alpha-1)^2+2f^0h(\sec\alpha-1), \tag{11}$$

$$\left.\frac{\partial^2U}{\partial\alpha^2}\right|_{\alpha=0}=2f^0h. \tag{12}$$

Clearly, if $f^0>0$, U is always greater than 0, and the $U(\alpha)$ is concave up around $\alpha=0$, that is, $x=0$, the equilibrium point, which indicates that the system is stable; if $f^0<0$, the system is unstable. We see that the results of the stability analysis can be obtained from both methods, and a spring system with a compressional pre-load is unstable around the equilibrium point, $\alpha=0$, consistent with our physical intuition. The pre-compressed two-spring structure expresses the instability of unconstrained negative-stiffness materials.

The stability analysis performed here is crucial for understanding the later analysis for extreme stiffness phenomena. In the following we will embed a negative stiffness element into other positive stiffness elements and investigate the system's unusual mechanical properties. Then, the stability analysis of a simplified spring model will be discussed.

III. ANALYSIS OF THE SPRING MODEL WITH EXTREME STIFFNESS

A. Linear model: No pre-load

To understand the influence of negative stiffness components on the overall stiffness of a mechanical system, we consider the two-dimensional spring system shown in Fig. 2. It can be seen that the negative stiffness element is the inner set of springs when they are deformed to the vertical position. (As demonstrated in Sec. II, the pre-compressed two-spring structure contains negative stiffness.) The springs are assumed to be linear, with force–displacement relations of the form $F=kx$, where k is a constant. Because the angles change with deformation, a complete load–displacement analysis requires us to adopt the equations of motion based on the deformed configuration, which is the central concept of geometrical nonlinear analysis (see Sec. III B). Geometrical nonlinear analysis is a method of characterizing load–displacement relations of a structure under a large deformation assumption.

We first perform a linear analysis in the absence of pre-load, to make a comparison with the geometrical nonlinear analysis presented later. The analysis is conducted using the energy method under the quasi-static assumption, that is, neglecting inertial terms. The total strain energy of the system is, in terms of the displacements x_a and x_b,

$$U=2U_1+U_2+2U_3, \tag{13}$$

where $U_1=k_1\,(x_b\sin\theta)^2$, $U_2=k_2\,(x_b-x_a)^2$, and $U_3=k_3\,(x_a\sin\phi)^2$. Here θ and ϕ are the angles of springs *bc* and *ac* from the vertical line, *bd*, indicating the initial configuration of the system. The subscripts 1, 2, and 3 denote the *bc* or *bd* spring, *ab* spring, and the *ac* or *ad* spring, respectively. In other words, the subscripts 1, 2, and 3 represent the springs with the spring constant, k_1, k_2, and k_3, respectively.

We now obtain the force displacement relation for the spring system. We can do so by a direct application of Newton's second law or by an energy method such as Castigliano's (first) principle,[17] which states that for linear elastic materials under small deformation, the partial derivative of the total strain energy with respect to an external force is equal to the displacement in the structure corresponding to that force. Specifically, $F_i=\partial U(x_j)/\partial x_i$, where i and j denote the direction of the generalized coordinates. The force–displacement relation for the system is

$$\begin{bmatrix} k_2+2k_3\sin^2\phi & -k_2 \\ -k_2 & k_2+2k_1\sin^2\theta \end{bmatrix}\begin{Bmatrix} x_a \\ x_b \end{Bmatrix}=\begin{Bmatrix} F_a \\ F_b \end{Bmatrix}. \tag{14}$$

We can use Eq. (14) and the pre-determined parameters of stiffness and initial geometry of the system to obtain a specific load–displacement relation of the system. With the assumption that the force $F_b=0$, the degrees of freedom of the system can be reduced from two to one. Equations (15) and (16) show explicitly the interrelation between the two degrees of freedom and the load–displacement relation at point *a*, respectively:

$$x_b=\frac{k_2}{k_2+2k_1\sin^2\theta}x_a, \tag{15}$$

$$x_a=\frac{k_2+2k_1\sin^2\theta}{2k_2k_3\sin^2\phi+2k_1k_2\sin^2\theta+4k_1k_3\sin^2\phi\sin^2\theta}F_a. \tag{16}$$

The ratio of F_a to x_a in Eq. (16) can be considered as the effective stiffness of the linearized system in the incremental sense. Equations (15) and (16) will be used to compare with the following analysis, which incorporates the effects of pre-load in a full nonlinear representation. Observe that as we might expect, all terms are positive and there are no singularities.

B. Geometrically nonlinear model including pre-load

We now analyze the spring model in Fig. 2 including the effects of pre-load in the context of full geometrical nonlinearity. The goal is to explore interesting phenomena in the vicinity of the snap-through of springs *bc* and *bd*. The static or dynamic equations of motion have to be expressed with respect to the deformed configuration in order to fulfill the requirement of geometrical nonlinear analysis. To derive the governing equations for the system, we introduce the kinematic relations first, then the equations of motion, and finally the constitutive equations.

1. Kinematic relations

We let the angles α and β represent the change of θ and ϕ after the deformation as shown in Fig. 2, and interpret α and β as generalized coordinates. The change of the lengths of the springs, denoted by Δ, can be related to the generalized coordinates as:

$$\Delta_1=\frac{h}{\cos(\theta-\alpha)}-\frac{h}{\cos\theta}, \tag{17}$$

$$\Delta_2=(h\tan(\phi-\beta)-h\tan(\theta-\alpha))-(h\tan\phi-h\tan\theta), \tag{18}$$

$$\Delta_3=\frac{h}{\cos(\phi-\beta)}-\frac{h}{\cos\phi}. \tag{19}$$

Once the relationship between the deformation of springs and the generalized coordinates is found, the total potential energy of the spring system, including the contribution from initial forces, shown in Eq. (20), will be used in the stability analysis of the elastic system in the absence of damping,[16]

$$U=k_1\Delta_1^2+\frac{1}{2}k_2\Delta_2^2+k_3\Delta_3^2+2\,f_1^0\Delta_1+f_2^0\Delta_2+2\,f_3^0\Delta_3+\frac{(f_1^0)^2}{k_1}+\frac{(f_2^0)^2}{2k_2}+\frac{(f_3^0)^2}{k_3}. \tag{20}$$

Here h is half of the vertical distance (the length of the line *cd*) between the two hinges. We can also see that the relation between the generalized coordinates and displacements at points *a* and *b* is

$$x_a=h\tan\phi-h\tan(\phi-\beta), \tag{21}$$

$$x_b=h\tan\theta-h\tan(\theta-\alpha). \tag{22}$$

2. Equations of motion

Newton's second law for the mass points *a* and *b* gives the following equations of motion in terms of the generalized coordinates $\alpha(t)$ and $\beta(t)$, and the displacements $x_a(t)$ and $x_b(t)$:

$$m_a\ddot{x}_a=F_a+f_2+2\,f_3\sin(\phi-\beta), \tag{23}$$

$$m_b\ddot{x}_b=2\,f_1\sin(\theta-\alpha)-f_2, \tag{24}$$

where f_1, f_2, and f_3 are the internal forces in the k_1, k_2, and k_3 springs, respectively, and m_a and m_b are the masses at points *a* and *b*, respectively. By substituting the kinematic relations, Eqs. (21) and (22), into Eqs. (23) and (24), the equations of motion can be expressed in terms of the generalized coordinates:

$$\mathbf{A}\begin{Bmatrix} \ddot{\alpha} \\ \ddot{\beta} \end{Bmatrix}+\mathbf{B}\begin{Bmatrix} \dot{\alpha}^2 \\ \dot{\beta}^2 \end{Bmatrix}=\begin{Bmatrix} 2\,f_1(t)\sin(\theta-\alpha)-f_2(t) \\ p_a+f_2(t)+2\,f_3(t)\sin(\phi-\beta) \end{Bmatrix}, \tag{25}$$

where

$$\mathbf{A}=\begin{bmatrix} m_bh\sec^2(\theta-\alpha) & 0 \\ 0 & m_ah\sec^2(\phi-\beta) \end{bmatrix}, \tag{26}$$

$$\mathbf{B}=\begin{bmatrix} -2m_b h\sec^2(\theta-\alpha)\tan(\theta-\alpha) & 0 \\ 0 & -2m_a h\sec^2(\phi-\beta)\tan(\phi-\beta) \end{bmatrix}. \tag{27}$$

3. Constitutive relations

Hooke's law holds for linearly elastic springs and the relation between force and deformation is linear, that is,

$$f_1=k_1\Delta_1+f_1^0, \tag{28}$$

$$f_2=k_2\Delta_2+f_2^0, \tag{29}$$

$$f_3=k_3\Delta_3+f_3^0, \tag{30}$$

where the f's are the total spring forces, and f^0's are the initial forces or pre-loads inside the springs. The sign convention of the internal forces is chosen so that tension is positive. If we substitute the constitutive equations into the equations of motion, we obtain the governing equations in the generalized coordinates:

$$\mathbf{A}\begin{Bmatrix}\ddot{\alpha}\\ \ddot{\beta}\end{Bmatrix}+\mathbf{B}\begin{Bmatrix}\dot{\alpha}^2\\ \dot{\beta}^2\end{Bmatrix}=\begin{Bmatrix} \dfrac{2k_1h\sin(\theta-\alpha)}{\cos(\theta-\alpha)}-\dfrac{2k_1h\sin(\theta-\alpha)}{\cos\theta}+2f_1^0\sin(\theta-\alpha)-[k_2(h\tan(\phi-\beta)-h\tan(\theta-\alpha)-h\tan\phi+h\tan\theta)+f_2^0] \\ F_a+[k_2(h\tan(\phi-\beta)-h\tan(\theta-\alpha)-h\tan\phi+h\tan\theta)+f_2^0]+\dfrac{2k_3h\sin(\phi-\beta)}{\cos(\phi-\beta)}-\dfrac{2k_3h\sin(\phi-\beta)}{\cos\phi}+2f_3^0\sin(\phi-\beta) \end{Bmatrix}. \tag{31}$$

If we assume quasi-static processes, the right-hand side of Eq. (31) is zero. Then Eq. (31) can be restated as the following equilibrium equations. The strategy used here is analogous to Eqs. (15) and (16) in the previously mentioned linear model, and the purpose is to relate the two generalized coordinates to the only applied load at point a,

$$\beta=\phi-\arctan\left(\tan\phi-\tan\theta+\tan(\theta-\alpha)-\frac{f_2^0}{k_2h}+2\frac{k_1}{k_2}\times\left(\frac{-\sin(\theta-\alpha)}{\cos\theta}+\tan(\theta-\alpha)+\frac{f_1^0}{k_1h}\sin(\theta-\alpha)\right)\right), \tag{32}$$

$$F_a=-(k_2h(\tan(\phi-\beta)-\tan(\theta-\alpha)+\tan\theta-\tan\phi)+f_2^0)-2\left(\frac{k_3h}{\cos(\phi-\beta)}-\frac{k_3h}{\cos\phi}+f_3^0\right)\sin(\phi-\beta). \tag{33}$$

The equilibrium equations (32) and (33) are responsible for generating load–displacement curves with no restriction on the magnitude of the displacements at nodes a and b.

IV. STABILITY ANALYSIS OF A SPRING MODEL WITH EXTREME STIFFNESS

The spring model in Sec. III is important for demonstrating how a negative stiffness element surrounded with positive stiffness elements leads to extreme overall stiffness. However, a direct investigation of its stability with the Routh–Hurwitz method involves mathematical and numerical complexity that might obscure the underlying physics, especially when viscosity is included. Here, we analyze the stability of a linear spring model, as shown in Fig. 3. It is equivalent (except for the addition of a viscous element) to that in Fig. 2 for small deformations about an equilibrium point. The negative stiffness due to the pre-load in the springs k_1 in Fig. 2 is subsumed as a linear negative spring in Fig. 3. Because stability analysis, based on Lyapunov's indirect theorem, deals with perturbations of a linearized system, there is no loss of generality.

The governing equations of the system in Fig. 3 can be directly written as follows, with $F_1=0$,

$$\begin{bmatrix} m_1 & 0 \\ 0 & m_2 \end{bmatrix}\begin{pmatrix}\ddot{x}_1\\ \ddot{x}_2\end{pmatrix}+\begin{bmatrix} k_1+k_2 & -k_2 \\ -k_2 & k_2 \end{bmatrix}\begin{pmatrix}x_1\\ x_2\end{pmatrix}+\begin{pmatrix}f\\ 0\end{pmatrix}=\begin{pmatrix}0\\ F_2\end{pmatrix}, \tag{34}$$

$$f+\frac{\eta}{\kappa_1+\kappa_2}\dot{f}=\frac{\kappa_1\kappa_2}{\kappa_1+\kappa_2}x_1+\frac{\kappa_1\eta}{\kappa_1+\kappa_2}\dot{x}_1. \tag{35}$$

Here η is the viscosity, and the k's and κ's represent the stiffness of the springs. The element parallel to the k_1 spring is often called a standard linear solid element in the context of viscoelasticity. To demonstrate that the system exhibits extreme stiffness, the compliance (that is, the ratio of the displacement to the applied force) of the system can be easily calculated in the frequency domain with the aid of a Fourier transformation:

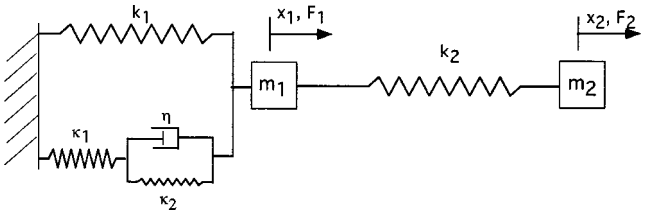

Fig. 3. One-dimensional linear spring system for demonstrating stability with a negative stiffness component. $k_1=10\times10^6$ N/m, and $k_2=5\times10^6$ N/m. Here κ_1, κ_2, and η form a standard linear solid element in the context of viscoelasticity. Assigning κ_1 to be negative is equivalent to compressional pre-load in the k springs in Fig. 1(b).

$$\begin{bmatrix} -\omega^2 m_1 + k_1 + k_2 + \dfrac{\kappa_1\kappa_2 + i\omega\kappa_1\eta}{\kappa_1 + \kappa_2 + i\omega\eta} & -k_2 \\ -k_2 & -\omega^2 m_2 + k_2 \end{bmatrix} \times \begin{pmatrix} \tilde{x}_1 \\ \tilde{x}_2 \end{pmatrix} = \begin{pmatrix} 0 \\ \tilde{F}_2 \end{pmatrix}. \tag{36}$$

The tilde denotes the Fourier transformed variables. If we let $\omega = 0$, we can obtain the compliance of the system under a quasi-static assumption.

For stability in the sense of Routh–Hurwitz, the equations of motion, Eqs. (34) and (35), can be rewritten in state space as

$$\begin{pmatrix} \dot{u}_1 \\ \dot{u}_2 \\ \dot{v}_1 \\ \dot{v}_2 \\ \dot{f} \end{pmatrix} = \mathbf{J} \begin{pmatrix} u_1 \\ u_2 \\ v_1 \\ v_2 \\ f \end{pmatrix} + \begin{pmatrix} 0 \\ 0 \\ 0 \\ \dfrac{F_2}{m_2} \\ 0 \end{pmatrix}, \tag{37a}$$

where

$$\mathbf{J} = \begin{bmatrix} 0 & 0 & 1 & 0 & 0 \\ 0 & 0 & 0 & 1 & 0 \\ -\dfrac{k_1 + k_2}{m_1} & \dfrac{k_2}{m_1} & 0 & 0 & -\dfrac{1}{m_1} \\ \dfrac{k_2}{m_2} & -\dfrac{k_2}{m_2} & 0 & 0 & 0 \\ \dfrac{\kappa_1\kappa_2}{\eta} & 0 & \kappa_1 & 0 & -\dfrac{\kappa_1 + \kappa_2}{\eta} \end{bmatrix}. \tag{37b}$$

Here $v_1 = du_1/dt$ and $v_2 = du_2/dt$. The second term on the right-hand side of Eq. (37a) is irrelevant to the stability analysis [see Eq. (2)]. The reason is that this term contributes a particular solution to the ordinary differential equation. As long as the driving force, F_2, is a bounded function or its driving frequency is not the natural frequency of the system (for $\eta = 0$), the contribution of the particular solution will not cause unbounded responses of the system. The inverse of the eigenvalue of the matrix **J** has the dimensions of time, so it can be interpreted as a time constant indicating the rate of the growth or decay of the response of the system. Therefore, the stability analysis will mainly investigate the eigenvalues of the **J** in Eq. (37).

V. RESULTS AND DISCUSSION

A. Stiffness at equilibrium points

In the following numerical simulations of the spring system in Fig. 2, we assume $h = 10\sqrt{3}$ mm, $\theta = 30°$, and $\phi = 60°$ as initial conditions. Pre-load in the spring k_2 will modify this geometry in the absence of an external force. Figure 4 shows the static characteristics of the mechanical spring system without the k_3 springs, based on Eqs. (21) and (22) for x_a and x_b and Eq. (33) for F_a in terms of the generalized coordinates, angles α and β. For $k_3 = 0$ in Fig. 2, the system is equivalent to a series (Reuss) composite cell. We remark that Lakes and Drugan[9] showed that this type of system is unstable if it is unconstrained. Geometrical nonlinearity is manifest in the calculation to include the effect of the change of structural shape, even though each spring has a linear force-deformation characteristic, because the angles change as the system is deformed. In the linear approximation, the system will never buckle due to the lack of consideration of geometrical changes, as the straight lines (see Fig. 4, curves denoted as ''Linear, no pre-load''). The match of the slopes of the load–displacement curves for the linear and geometrical nonlinear analysis near zero deformation confirms the validity of our calculation. By tuning the stiffness of the k_2 springs, it can be seen that the overall stiffness of the system at point *a*, the loading point, approaches infinity around $x_a = 10$ mm when $k_1 = 10$ and $k_2 = 3 \times 10^6$ N/m. If we observe the curves for $k_2 < 3 \times 10^6$ N/m, it is understood that the corresponding functions for the curves are multivalued functions with respect to both displacement and loads.

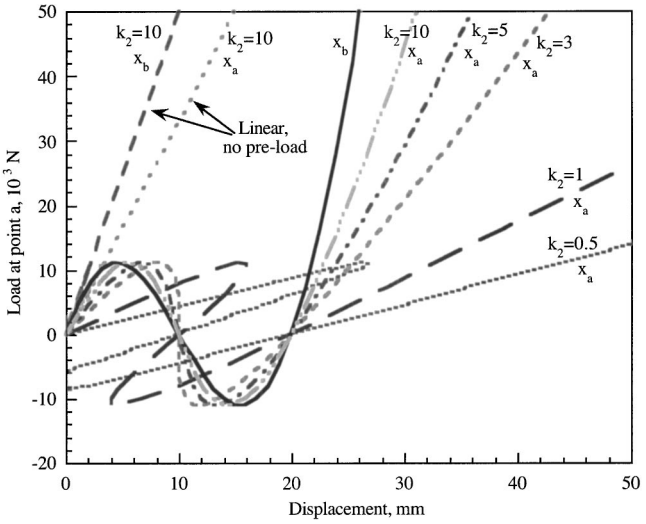

Fig. 4. Load–displacement diagram for the spring system in Fig. 2 with no k_3 springs and no initial forces. The spring constant for k_1 is 10×10^6 N/m. The symbols x_a and x_b indicate the displacement at points *a* and *b*, respectively. The curved lines are calculated results based on the geometric nonlinear analysis with no pre-load. The straight lines represent a linear approximation about zero displacement. The units for k_2 in the diagram are 10^6 N/m.

The snap-through or back-through phenomena will occur in both the numerical simulations by solving Eqs. (23) and (24) with the Newton–Raphson method[2] and the laboratory experiments if we try to control either the displacement or the loading at point *a*. However, in this case, by controlling the generalized coordinate α by hand, the curves can be numerically constructed with a one-to-one relation between α and the linear displacement x_a, and α and the loading F_a through Eqs. (32) and (33).

We next include the k_3 springs so that the snap-through can occur in the vicinity of zero applied load. Figures 5 and 6 show the post-buckling behavior of the system with nonzero k_3 elements. There are two possible buckling phenomena when $k_3 \neq 0$. One is the inner springs (k_1) undergoing snap-through, and the other is the buckling of the outer springs (k_3). Based on the chosen parameters, the extreme overall stiffness occurs at the snap-through of the inner springs. As shown in Fig. 6, under the chosen pre-load condition, tuning k_3 will not increase the infinite-stiffness region, but will change the characteristics of the transition from normal-stiffness to extreme-stiffness.

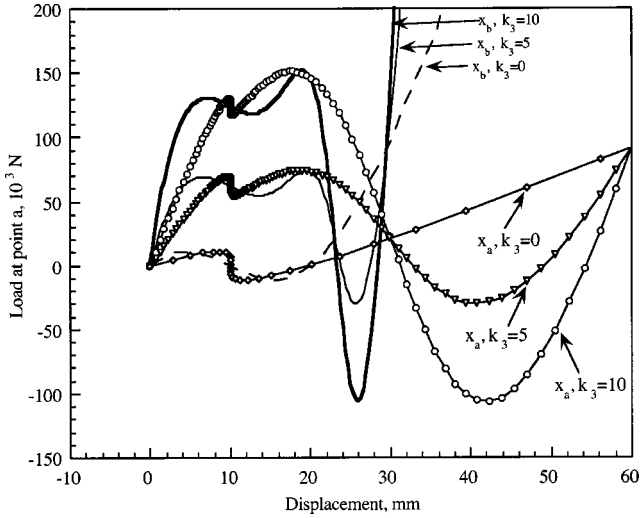

Fig. 5. The load–displacement diagram for spring system in Fig. 2 with k_3 springs varied, and no pre-load. The spring constants for k_1 and k_2 are 10 and 3×10^6 N/m, respectively. The units for k_3 are 10^6 N/m.

It is understood that each of the initial forces, f_1^0, f_2^0, and f_3^0, is a free parameter: there are no equations relating them. If we specify the initial forces, the spring forces f_1, f_2, and f_3 will change, and the geometry of the system will also change. A nonzero f_2^0 as chosen here causes the geometry of the system to change accordingly. The same effect also could be obtained by changing the initial configuration of the system, that is, adjusting θ and ϕ directly, with nonzero initial forces inside all the springs. Figure 7 shows the initial shape and the deformed shape (after pre-load) of the spring model. After applying the pre-load, f_2^0, and before applying any load at point a we can see that the system is deformed from the $abcd$ to the $a'b'cd$ configuration. Therefore, before F_a is applied, there are nonzero forces in all the springs. Also, Fig. 7 shows two other equilibrium configurations corresponding to $F_a=0$, indicated by double- and triple-primed symbols, in which the double-primed symbols indicate that the system exhibits extreme high effective stiffness at point a.

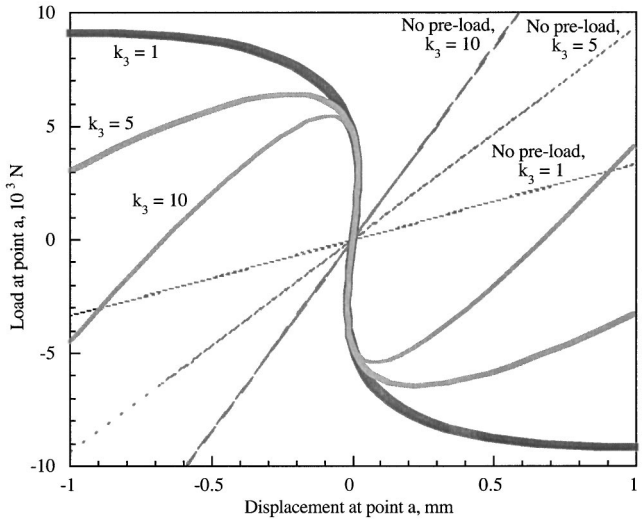

Fig. 6. The load–displacement diagram for the spring system in Fig. 2 with pre-load: the initial forces are $f_1^0=0$, $f_2^0=-30\times10^3$ N, and $f_3^0=0$ with initial $\theta=30°$ and $\phi=60°$. The values of k_1 and k_2 are 10 and 3×10^6 N/m, respectively. The units for k_3 are 10^6 N/m. The straight line solutions, corresponding to no pre-load, are obtained from Eqs. (15) and (16).

B. Stability

For purely elastic cases, we can investigate the stability of the critical equilibrium position of the spring model in Fig. 2 by the energy method. Equation (20) is plotted as a surface in Fig. 8 with respect to the displacements at points a and b. The parameters are $k_1=10$, $k_2=3$, $k_3=5\times10^6$ N/m, $f_1^0=0$, $f_2^0=-30\times10^3$ N, $f_3^0=0$, $\theta=30°$, and $\phi=60°$. The magnitude of the masses m_1 and m_2 is irrelevant to the calculation because of the quasi-static assumption. We see that the surface has a saddle shape at the critical equilibrium point, $x_a=0$ mm and $x_b=10$ mm. It is understood that the system is not stable at the saddle point as discussed in Ref. 9. The system is not necessarily free to have any values of the coordinates x_a and x_b; it is constrained by the equilibrium equations. For example, applying Eq. (32) gives a concave-up section of the saddle, which suggests stability in the presence of perturbations in the force F_a. However, the application of Eq. (33) with $F_a=0$ gives a concave-down section of the saddle surface in Fig. 8, indicating instability in the presence of perturbations of F_b. Both degrees of freedom must be considered in an energy approach to determine the stability of this system.

It is not realistic to draw definite conclusions about the stability from purely elastic models because in real materials, viscoelastic effects cannot be neglected. Nonetheless, the equilibrium points with locally minimal energy before and after snap-through are stable in accordance with Dirichlet's theorem,[12] which states an equilibrium point is stable if the energy of the system reaches a minimum. To probe the stability of this extreme phenomenon including considerations of viscoelasticity, we focus on the behavior of the linearized spring model in Fig. 3. In the calculation the parameters are $k_1=10\times10^6$ N/m, $k_2=5\times10^6$ N/m, $\kappa_2=5\times10^6$ N/m, and $m_1=m_2=10^{-12}$ kg. Compliances are calculated under the assumption of zero frequency ($\omega=0$) to represent a quasi-static deformation. The values for the masses will not change the compliance calculation due to the quasi-static assumption, but will strongly influence the eigenvalue calculation. Figure 9 shows the familiar resonant- and anti-resonant-like compliance curves, signatures of a system with negative inclusions, when κ_1 is tuned to be negative.

Because the frequency is assumed to be zero (static equilibrium), the effects are not resonant. The response of the spring model resembles that of a resonating system because the inertial terms in a classic mass–spring system are opposite in sign from the elastic terms. At sufficiently high frequency, the negative effective stiffness associated with the inertial terms suffices to cancel the elastic terms, giving rise to resonant behavior; for a system with more than one degree of freedom, anti-resonance occurs as well. The frequency dependence and the negative sign in this case arise from the second derivative of the displacement in Newton's second law. By contrast, the negative stiffness of a negative spring has no frequency dependence. The frequency dependence can however be introduced in negative spring systems by the inclusion of viscous elements, and will be briefly discussed later.

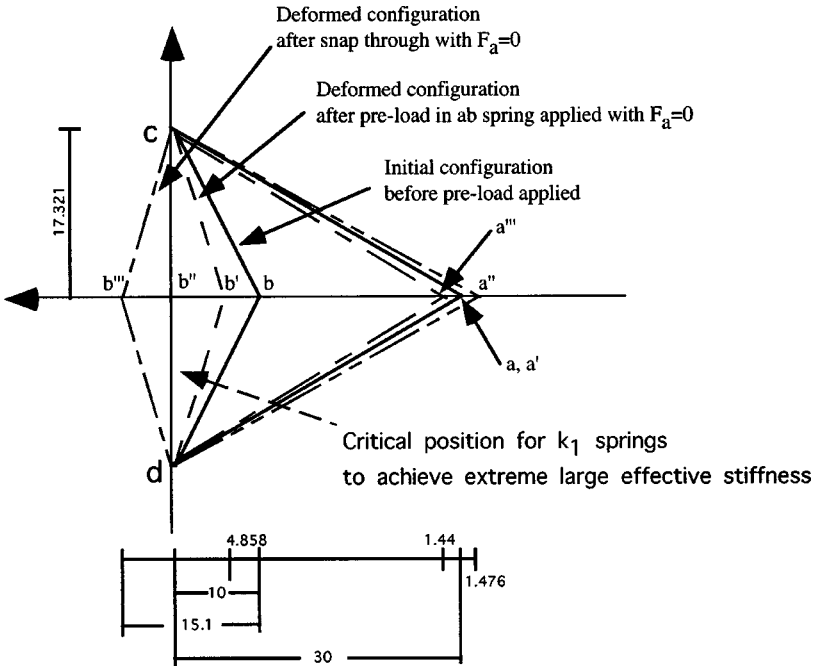

Fig. 7. The change in the geometry of the spring system in Fig. 2 with pre-load in spring 2 (dimensions in millimeters). The un-primed symbols indicate the initial configuration before the f_2^0 pre-load is applied, the single-primed symbols indicate the deformed shape after the only pre-load is applied. Double-primed symbols indicate the deformed shape for extreme large stiffness; triple-primed the deformed shape after snap-through.

The compliance between resonant and anti-resonant-like peaks in Fig. 9 is negative. Also, it is understood that the compliance at node 2 can be considered as the effective compliance of the system as a whole. At zero frequency, the magnitude of the viscosity will not change the compliance calculation, as can be seen in Eq. (36). The lowest compliance indicates the highest stiffness and vice versa. Based on the numerical resolution adopted in this analysis, which is determined by a pre-chosen increment for the tuning parameter, κ_1, the highest overall stiffness around the anti-resonant-like peak ($\kappa_1 \approx -3.7\times10^6$ N/m) is about 20 times greater than that with positive κ_1. Theoretically, the overall stiffness can reach infinity due to the presence of negative stiffness elements. At $\kappa_1 \approx -3.2\times10^6$ N/m, the system reaches its highest compliance because the amount of negative stiffness neutralizes that of the positive stiffness element in element 1 to the left in Fig. 2. It is not surprising that the highest peaks of both compliance curves occur at the same amount of negative stiffness in element 1 because the stiffness of this element dominates the relative motion of the nodes to the fixed end. Also in Fig. 9, we can see the stability of the system from the trajectories of the only eigenvalue with a positive real part. The eigenvalues are calculated from Eq. (37). Figure 9(b) is an expanded version of Fig. 9(a) for the trajectories of the eigenvalue. It can be seen that when $\kappa_1 > -3.2\times10^6$ N/m, the system is stable for various viscosities because there are no eigenvalues with a positive real part. Although there is an eigenvalue with non-negative real part when $\kappa_1 \leqslant -3.2\times10^6$ N/m, its magnitude can be made to be as small as desired by increasing the viscosity in the system. Therefore, around the point of interest ($\kappa_1 \approx -3.7\times10^6$ N/m), which gives rise to extreme positive overall stiffness, the system is in a metastable state. The root-locus plot of all eigenvalues with $\eta=10$ and $\eta=100\times10^6$ ($\mathrm{N\,m^{-1}\,s}$), respectively, is shown in Fig. 10(a). The arrows indicate the direction of the movement of the eigenvalues with respect to the tuning parameter, η. A detailed root-locus plot for the only eigenvalue with a positive real part is shown in Fig. 10(b). Again, the system is metastable because the only eigenvalue with a positive real part can be made small by a choosing a high viscosity.

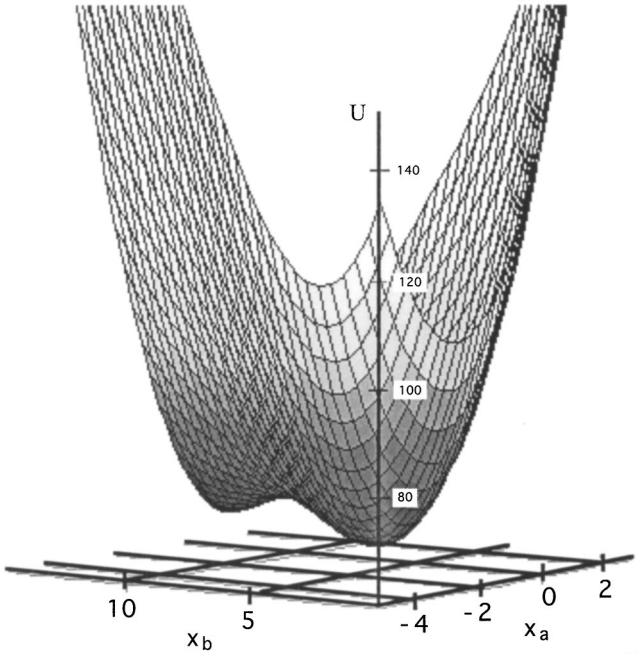

Fig. 8. Two-dimensional energy landscape of the spring model in Fig. 2 with respect to x_a and x_b with no force at point a or b. $k_1=10\times10^6$, $k_2=3\times10^6$, $k_3=5\times10^6$ N/m, $f_1^0=0$, $f_2^0=-30\times10^3$ N, and $f_3^0=0$.

As for the frequency response of the effective overall dynamic compliance, that is, the dynamic compliance at node 2, Fig. 11(a) shows the results of the calculation assuming that $\eta=10\times10^6$ ($\mathrm{N\,m^{-1}\,s}$) and $\kappa_2/\kappa_1=-5$, with various κ_1. It can be seen that for this set of parameters, when $\kappa_1=-15\times10^6$ N/m, the overall dynamic stiffness dramatically increases as the frequency increases. However, when $\kappa_1=-10\times10^6$ N/m, the overall dynamic stiffness decreases with

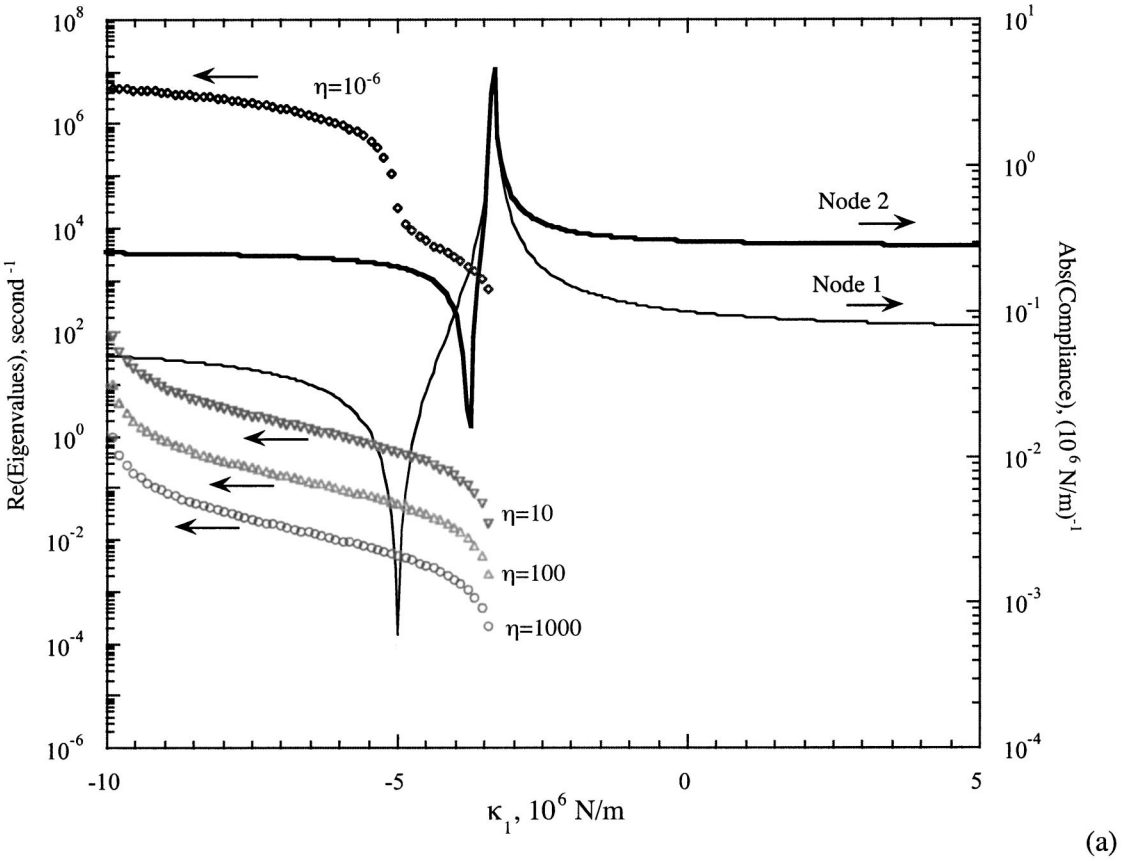

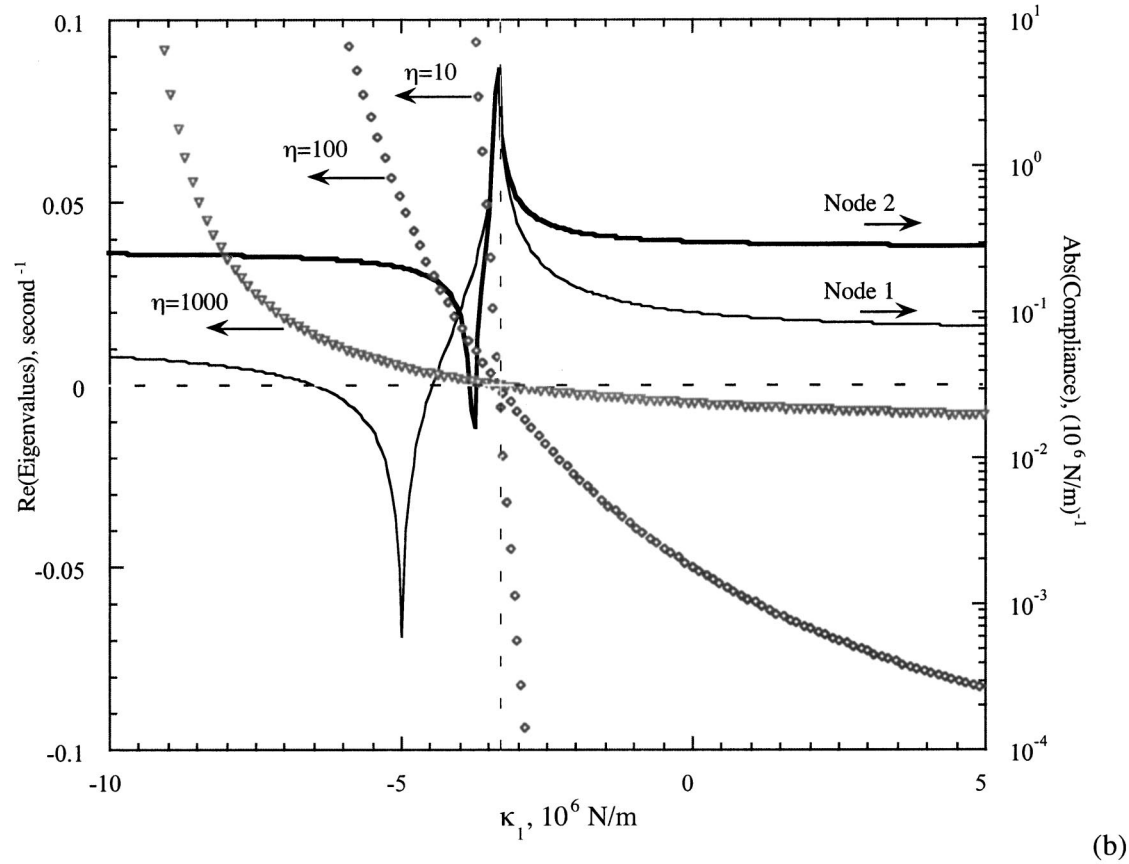

Fig. 9. Compliance and stability analysis of the spring model in Fig. 3. $k_1=10\times10^6$, $k_2=5\times10^6$, and $\kappa_2=5\times10^6$ N/m are fixed parameters. (a) Eigenvalues on log scale. (b) Eigenvalues on linear scale showing sign change at the critical κ_1. Data for $\eta=10^{-6}$ are omitted. The viscosity η is in units of 10^6 N m^{-1} s. Increasing the viscosity decreases the degree of instability. The eigenvalues are calculated from Eq. (37). The compliances are calculated from Eq. (36) with $\omega=0$.

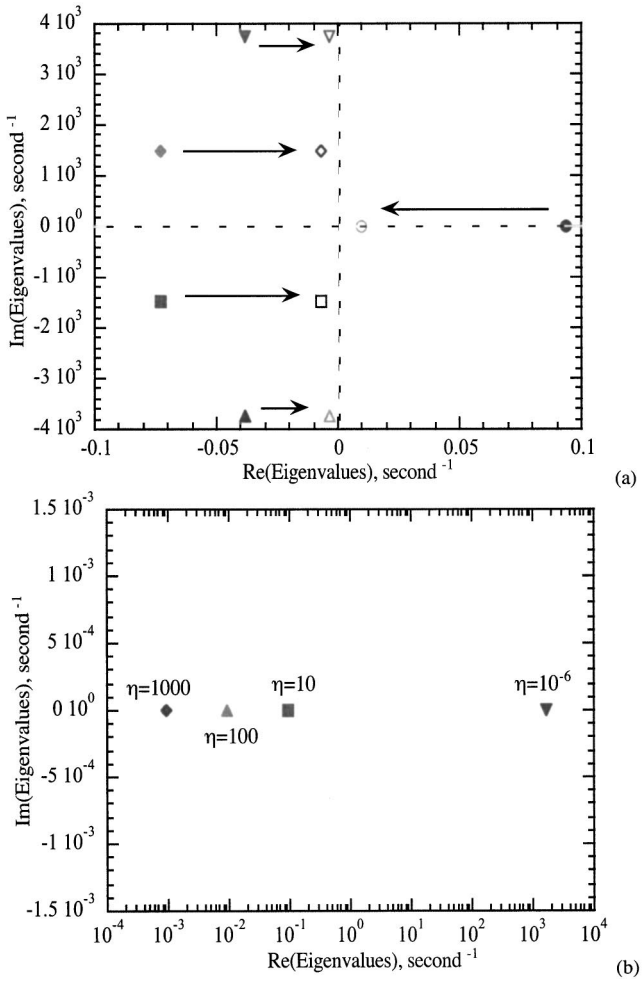

Fig. 10. Root-locus plots with the tuning parameter, η, around the extreme high stiffness state. $k_1=10\times10^6$, $k_2=5\times10^6$, $\kappa_1=-3.7\times10^6$, and $\kappa_2=5\times10^6$ N/m. (a) All eigenvalues. Closed symbols: $\eta=10$; open symbols: $\eta=100$. The viscosity η is in units of 10^6 N m^{-1} s. The arrows indicate the increase of η. (b) Trajectory of the only eigenvalue with a positive real part. Stability corresponds to the real part (Re) of all eigenvalues less than zero. Instability corresponds to the real part of an eigenvalue greater than zero. A sufficiently small positive real part of an eigenvalue corresponds to metastability.

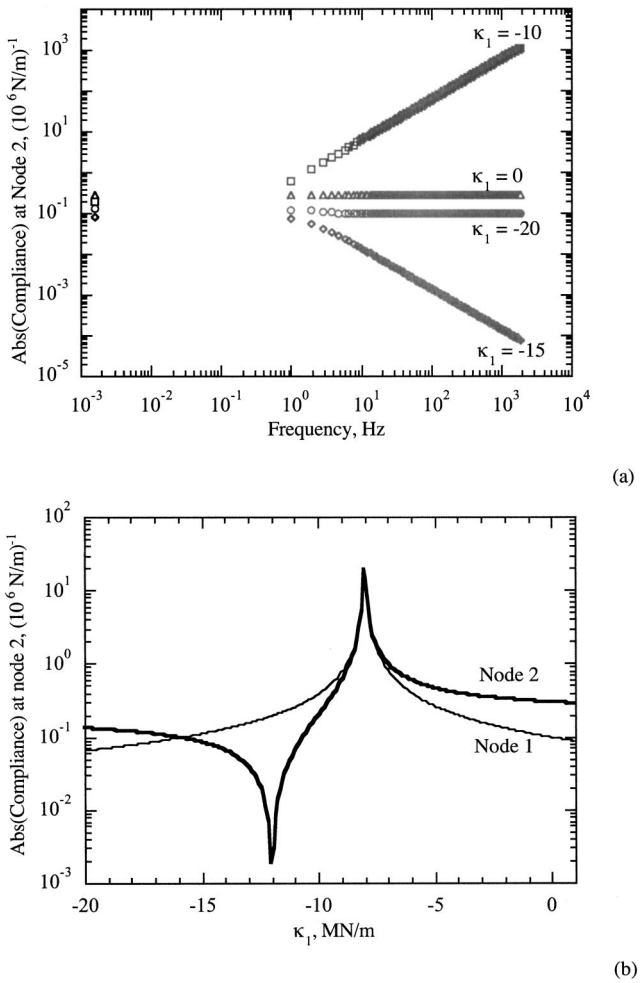

Fig. 11. (a) Compliance vs frequency with various κ_1 for the spring model in Fig. 3 with $\eta=10\times10^6$ (N m^{-1} s) and $\kappa_2/\kappa_1=-5$. κ's are in units of 10^6 N/m. (b) Quasi-static compliance of model in Fig. 3 with $\kappa_2/\kappa_1=-5$.

frequency. The increase or decrease of the dynamic stiffness with frequency is due to the response of the viscous element and is not due to inertial effects, because the masses are assumed to be 10^{-12} kg in the calculation. In addition, the frequency dependence is minimal when the amount of negative stiffness is small (for example, $\kappa_1=0$) or large (for example, $\kappa_1=-20\times10^6$ N/m) in the calculated frequency range. For comparison, with the same assumption, that is, $\kappa_2/\kappa_1=-5$, the corresponding quasi-static response is shown in Fig. 11(b) as a function of κ_1. The value of the node 2 compliance between the resonant-like and anti-resonant-like peaks is negative, and compliance of node 1 is negative for κ_1 less than that corresponding to the peak (that is, $\kappa_1\approx-7\times10^6$ N/m). The stability of the system at a certain frequency has the same characteristics as that analyzed before under the quasi-static assumption. In other words, driving the system with a sub-resonant frequency will not increase or decrease the degree of stability of the system. As mentioned, the presence of a sinusoidal driving force will not change the nature of stability when the applied force is bounded in the time domain and its frequency is not the natural frequency of the system.

VI. SUMMARY

As expected, agreement between the linear and geometric nonlinear analysis for small displacement is observed. By a rigorous geometric nonlinear analysis, the effect of a preload contributing to negative stiffness was identified. In this way the idea of using a negative value for the stiffness in Hooke's law was presented. Changing initial configurations of the model, such as θ, ϕ, or the stiffness of the springs, in the geometrical nonlinear analysis will not eliminate the extreme behavior, provided we choose different values for the free tuning parameters, the pre-loads. The results of the geometric nonlinear analysis verify the possibility of achieving extreme stiffness system with negative stiffness components. Theoretically, the effective stiffness can approach infinity.

An unconstrained negative stiffness element is unstable. Rigorous stability analysis via the energy method and Lyapunov's indirect method reveals that the present elastic model of spring networks with a negative stiffness element is

stable at the equilibrium point when tuned for extreme high compliance, but is not stable when tuned for extreme high stiffness. However, the unstable model can be made metastable (an arbitrarily long time constant for divergence) with the aid of a nonzero viscosity.

It is well known that natural diamond is in a metastable state at ambient conditions. Ultimately diamond is expected to become graphite (which has a lower energy state) with a large time constant of many years. In the present spring system, the time constant for divergence, when tuned to be metastable, can be made to be arbitrarily long. Therefore, a system with extreme overall stiffness due to a negative stiffness element is metastable. This analysis applies only to the present spring system. The behavior of general systems with negative stiffness constituents remains to be explored to determine the necessary and sufficient conditions for extreme mechanical behavior.

A negative stiffness element (containing springs with compressive pre-load), though unstable by itself, can be stabilized by including it in a system of positive stiffness elements. It is possible in such a system to achieve high compliance and high internal deformation (greater than the applied deformation) and to retain stability. This behavior may be of interest in the context of composites with extreme piezoelectric or thermal expansion coefficients.[11] The linear and geometrically nonlinear analyses agree in the limit of small deformation. The spring system also can exhibit arbitrarily high stiffness greater than that of any of the springs. Under these conditions the spring system is unstable, but if viscous elements are included, it can be made metastable with an arbitrarily long time constant for divergence. Furthermore, the quasi-static stiffness of the viscous damped system with an appropriate negative stiffness constituent tends to infinity with increasing frequency of the applied excitations.

[a)]Electronic mail: lakes@engr.wisc.edu

[1]J. M. Gere, and S. P. Timoshenko, *Mechanics of Materials* (Chapman & Hall, London, 1991), 3rd ed.

[2]K. J. Bathe, *Finite Element Procedures* (Prentice–Hall, Englewood Cliffs, NJ, 1996).

[3]G. Puglisi and L. Truskinovsky, ''Mechanics of a discrete chain with bistable elements, '' J. Mech. Phys. Solids **48**, 1–27 (2000).

[4]R. S. Lakes, ''Foam structures with a negative Poisson's ratio,'' Science **235**, 1038–1040 (1987).

[5]R. S. Lakes, ''Advances in negative Poisson's ratio materials,'' Adv. Mater. (Weinheim, Ger.) **5**, 293–296 (1993).

[6]R. S. Lakes, ''Extreme damping in compliant composites with a negative stiffness phase,'' Philos. Mag. Lett. **81**, 95–100 (2001).

[7]R. S. Lakes, ''Extreme damping in composite materials with a negative stiffness phase,'' Phys. Rev. Lett. **86**, 2897–2900 (2001).

[8]R. S. Lakes, T. Lee, A. Bersie, and Y. C. Wang, ''Extreme damping in composite materials with negative stiffness inclusions,'' Nature (London) **410**, 565–567 (2001).

[9]R. S. Lakes and W. J. Drugan, ''Dramatically stiffer elastic composite materials due to a negative stiffness phase?,'' J. Mech. Phys. Solids **50**, 979–1009 (2002).

[10]B. Paul, ''Prediction of elastic constants of multiphase materials,'' Trans. AIME **218**, 36–41 (1960).

[11]Y. C. Wang and R. S. Lakes, ''Extreme thermal expansion, piezoelectricity, and other coupled field properties in composites with a negative stiffness phase,'' J. Appl. Phys. **90**, 6458–6465 (2001).

[12]H. Leipholz, *Stability Theory: An Introduction to the Stability of Dynamic Systems and Rigid Bodies* (Wiley, New York, 1987), 2nd ed.

[13]J. E. Marsden and T. S. Ratiu, *Introduction to Mechanics and Symmetry* (Springer-Verlag, New York, 1994).

[14]D. R. Merkin, *Introduction to the Theory of Stability* (Springer-Verlag, New York, 1997).

[15]L. Meirovitch, *Methods of Analytical Dynamics* (McGraw–Hill, New York, 1970).

[16]D. Iesan, *Prestressed Bodies* (Addison–Wesley–Longman, 1989).

[17]Y. C. Fung, *Foundations of Solid Mechanics* (Prentice–Hall, Englewood Cliffs, NJ, 1965).